

Development and Application of Flow-Cytometric Techniques for Analyzing and Sorting Endospore-Forming Clostridia^{∇†}

Bryan P. Tracy,¹ Stefan M. Gaida,² and Eleftherios T. Papoutsakis^{3,4*}

Department of Chemical and Biological Engineering, Northwestern University, Evanston, Illinois 60208-3120¹; Department of Bioprocess Engineering, Institute of Biotechnology, Technical University of Berlin, Berlin, Germany²; Department of Chemical Engineering, Colburn Laboratory, University of Delaware, Newark, Delaware 19716³; and Delaware Biotechnology Institute, University of Delaware, Newark, Delaware 19711⁴

Received 15 July 2008/Accepted 7 October 2008

The study of microbial heterogeneity at the single-cell level is a rapidly growing area of research in microbiology and biotechnology due to its significance in pathogenesis, environmental biology, and industrial biotechnologies. However, the tools available for efficiently and precisely probing such heterogeneity are limited for most bacteria. Here we describe the development and application of flow-cytometric (FC) and fluorescence-assisted cell-sorting techniques for the study of endospore-forming bacteria. We show that by combining FC light scattering (LS) with nucleic acid staining, we can discriminate, quantify, and enrich all sporulation-associated morphologies exhibited by the endospore-forming anaerobe *Clostridium acetobutylicum*. Using FC LS analysis, we quantitatively show that clostridial cultures commonly perform multiple rounds of sporulation and that sporulation is induced earlier by the overexpression of Spo0A, the master regulator of endospore formers. To further demonstrate the power of our approach, we employed FC LS analysis to generate compelling evidence to challenge the long-accepted view in the field that the clostridial cell form is the solvent-forming phenotype.

Microbiology traditionally focused on analyzing microbes at the population scale, limiting conclusions about individual cell behavior to culture-level data (4). However, it is well accepted that microbial cultures, even clonal populations, exhibit more cellular heterogeneity than previously appreciated (1, 2, 6, 12, 13, 35). The study of culture heterogeneity is a relatively new field of microbiological research very significant to endospore-forming bacteria, notably clostridia.

Clostridia are obligate anaerobe, gram-positive, sporulating firmicutes that include pathogenic species significant to human/animal health and physiology and nonpathogenic species relevant to the commercial conversion of renewable resources into biofuels and commodity chemicals (26). Pathogenic species such as *Clostridium botulinum*, *C. difficile*, *C. perfringens*, and *C. tetani* produce 18% of all known bacterial toxins, making it the “most toxic” bacterial genus (28). Cellulolytic and solventogenic species such as *C. thermocellum*, *C. saccharobutylicum*, *C. cellulolyticum*, and *C. acetobutylicum* are some of the best-studied biomass-metabolizing bacteria, with significant potential for sustainable biofuel production via consolidated bioprocessing (23, 24). Nontoxic, proteolytic species, namely, *C. sporogenes* and *C. novyi*, are being engineered into promising chemotherapeutic vehicles, a process called clostridium-directed enzyme prodrug therapy (CDEPT) (25). CDEPT entails the intravenous delivery of clostridial spores, which infiltrate and selectively germinate in the hypoxic regions of solid tumors. The vegetative clostridia then produce an enzyme

that acts upon a prodrug precursor, converting it into its toxic form (25).

Central to all these fields of research is sporulation, which occurs in all clostridia in response to still largely unknown signals (26). Sporulation is directly linked genetically to CPE enterotoxin and C2 toxin expression in *C. perfringens* and *C. botulinum* (11), respectively. Sporulation is the very reason why *C. sporogenes* and *C. novyi* can be administered systemically for CDEPT, and sporulation is believed to be genetically coupled to the solvent metabolism of industrial organisms such as *C. acetobutylicum* (19). Although significant advances are being made (19), clostridial sporulation remains largely uncharacterized due in part to culture heterogeneity. Only a small portion of a typical culture sporulates for many of the most-studied species (14, 22, 27, 43). Thus, genetic, proteomic, and metabolic analyses are often complicated by culture heterogeneity.

Prior efforts at single-cell analysis of clostridial cultures include Fourier transform infrared spectroscopy, Raman spectroscopy coupled with microscopy, and electro-optical measurements (20, 30–33). Although powerful, these techniques are not capable of high-throughput analysis, are less capable of quantifying bulk population heterogeneity, are unable to enrich phenotypes for subsequent analyses, and often require custom-made equipment. Flow cytometry (FC) is a high-throughput, multiparametric analysis technique capable of discriminating and sorting individual cells. Although microbial FC analysis has been advancing for nearly half a century (35), it is employed to a very low extent for microbial compared to mammalian cell culture analysis. Bacteria are approximately 3 orders of magnitude smaller in mass and contain much less DNA, RNA, and protein per cell than mammalian cells (34). Thus, bacterial light scattering (LS) occurs at or near the threshold level of instrumental noise, and fewer fluorescently

* Corresponding author. Mailing address: 15 Innovation Way, Newark, DE 19711. Phone: (302) 831-8376. Fax: (302) 831-7090. E-mail: Papoutsakis@dbi.udel.edu.

† Supplemental material for this article may be found at <http://aem.asm.org/>.

∇ Published ahead of print on 17 October 2008.

labeled molecules per cell complicate fluorescence detection while increasing sample variance (34). Additionally, there are far fewer established assays that can be employed across all classes of bacteria due to the enormous heterogeneity among them. For example, there are many reports of ambiguous cell viability results with the increasingly popular Live/Dead BacLight viability assay from Invitrogen (3, 17, 36). Furthermore, many interesting bacterial species, including all clostridia, are difficult to genetically modify. Lastly, these are obligate anaerobes, and thus fluorescent proteins like green fluorescent protein cannot be employed due to strict requirements for oxygen (39).

Here we report the development of FC and fluorescence-assisted cell-sorting (FACS) methods for investigating clostridial sporulation and culture heterogeneity. We demonstrated the superior multiparametric detection, high-throughput, and sorting advantages of these techniques. We discriminated, quantified, and enriched all sporulation-associated morphologies, discussed in detail elsewhere (19). We validated our assays by analyzing and sorting batch cultures of wild-type (WT) *C. acetobutylicum* ATCC 824 and mutant or recombinant strains (8, 15, 40). We sorted all sporulation-associated cellular morphologies for microscopic analyses and developed a novel assay for determining the metabolic state of clostridial cultures. Finally, we demonstrated the utility of our methods by correlating FC-detected morphology changes with bulk-phase metabolite concentrations and generated compelling evidence to challenge the long-accepted view in the field that clostridial-form cells are responsible for solventogenesis (18).

MATERIALS AND METHODS

Bacterial strains and plasmids. Bacterial strains employed in this study were *C. acetobutylicum* ATCC 824 (ATCC, Manassas, VA) and the degenerate strain M5 (which has lost the 192-kb, 176-gene megaplasmid pSOL1) (5, 8). Plasmids employed were pSOS95del (MLS^r [macrolide-lincosamide-streptogramin B resistance], ColE1 origin of replication, repL [pIM13 origin of replication], Amp^r [ampicillin resistance], *thl* promoter) (40) and the Spo0A expression plasmid pMSP00A (Amp^r, MLS^r, ColE1 origin of replication, repL, carries *spo0A*) (15).

Growth conditions and maintenance. *C. acetobutylicum* ATCC 824 and recombinant strains were grown anaerobically in liquid clostridial growth medium (CGM) and solid 2× yeast-tryptone-glucose (pH 5.8) (2×YTG) at 37°C (42). CGM contained 80 g/liter glucose and was buffered with 30 mM sodium acetate (pH 7.0). 2×YTG contained 15 g/liter glucose. Recombinant strains were selected for and maintained under erythromycin pressure (100 µg/ml for liquid and 40 µg/ml for solid). Clostridial strains were stored at -85°C in fresh CGM supplemented with 15% glycerol and revived by anaerobic plating on 2×YTG. For spore-forming strains, colonies were grown for at least a week on 2×YTG and then heat shocked at 80°C for 10 min in CGM. Heat shocking was performed to kill all vegetative cells, to induce spore germination, and to insure the presence of pSOL1. Two hundred fifty-milliliter static flask cultures were used for all experiments, which were inoculated with a 4% (vol/vol) mid-exponential growth phase (absorbance at 600 nm [A_{600}] of ~0.6) culture.

Analytical methods. Cell growth was monitored by measuring optical A_{600} with a BioMate 3 series spectrophotometer (Thermo Spectronic, Rochester, NY). Culture supernatants were analyzed for glucose, acetate, butyrate, butanol, acetone, ethanol, and acetoin via a Waters (Milford, MA) high-performance liquid chromatograph (38).

FC analysis. FC analysis was performed on a BD LSRII FC (Franklin Lakes, NJ) equipped with three excitation lasers and eight-color detection. Specifically, the lasers were purple ($\lambda = 406$ nm, 50 mW), blue ($\lambda = 488$ nm, 25 mW), and red ($\lambda = 633$ nm, 17 mW). Forward-scatter characteristics (FSC) and side-scatter characteristics (SSC) were detected as small- and large-angle scatters of the 488-nm laser, respectively (35). Syto9 and propidium iodide (PI) were both excited by the 488-nm laser. PI was detected by a 685-nm long-pass and a 695/40-nm band-pass filter set. Syto9 was detected by a 505-nm long-pass, 530/

30-nm band-pass filter set. All analyses were performed while thresholding on SSC to remove noise.

FACS. Sorting was performed on a DakoCytomation MoFlo by the Northwestern University Robert H. Lurie Cancer Center FC Core Facility and on a FACSaria. Cells were sorted into two or four channels, and purity was evaluated immediately after sorting. Staining protocols and sample preparations were scaled up 10× in order to obtain enough sample for sorting. Samples were diluted to ~10⁹ cells/ml in 5 to 6 ml of 1% NaCl. Sorted cells were captured in 15-ml Falcon tubes for two-channel sorting and in 10-ml FC tubes for four-channel sorting. The sample injection port and sample collection apparatus were both maintained at 4°C. The final concentration of sorted cells was much lower than the sample concentration—these values were ~10⁵ to 10⁶ cells/ml versus ~10⁹ cells/ml—and total volumes were on average 25 to 50 ml. Subsequently, staining characteristics were lost after sorting due to the low concentration of dyes, as confirmed by microscopy and FC. Sorted populations were pelleted by a 15-min, 25,000 × *g* centrifugation. Pellets were resuspended in 3 to 10 µl depending on pellet size.

LS sample preparation. Samples for FC LS analysis were prepared by pelleting 500 µl of culture via a 1-min centrifugation at 16,000 × *g*. The supernatant was discarded and cells were washed by resuspension in 1 ml of sterile filtered 1% (wt/vol) NaCl. Cells were pelleted again and then resuspended in 40 µl of sterile filtered 1% (wt/vol) NaCl. This is the same protocol for preparing cell samples for nucleic acid (NA) staining analysis. The LS sample was prepared by diluting 1 to 5 µl of washed cells in 1 ml of sterile filtered 1% (wt/vol) NaCl.

NA staining protocol. For an A_{600} of <0.5, 1 ml of culture was sampled. For an optical density at 600 nm of >0.5, 0.5 ml of culture was sampled. Cells were washed and prepared as described for LS samples. The 40 µl of washed cells was diluted to a final volume of 200 µl with sterile filtered 1% (wt/vol) NaCl. The Invitrogen Live/Dead BacLight bacterial viability stain was employed. Syto9 and PI were mixed to final solution concentrations of 1.67 mM and 9.985 mM, respectively. Two microliters of Syto9-PI mix was added to the 200-µl sample, and this was mixed via vortexing and incubated at room temperature in the dark for 10 min. The stained cells were then pelleted by centrifugation for 1 min at 16,000 × *g* and washed again in 1 ml of sterile filtered 1% (wt/vol) NaCl. Samples were finally resuspended in 40 µl of sterile filtered 1% (wt/vol) NaCl. The FC sample was prepared by diluting 1 to 5 µl of washed cells in 1 ml of sterile filtered 1% (wt/vol) NaCl and immediately analyzed on the FC.

Phase-contrast and fluorescence microscopy. Phase-contrast and fluorescence microscopy slides were prepared by pipetting 1-µl portions of the washed 20-µl cell suspension on the centers of glass microscope slides and covering with glass coverslips. Phase-contrast and fluorescence microscopy were performed with a Leica DM IRE2 inverted fluorescence microscope (Wetzlar, Germany). Magnification was accomplished with a 63× oil immersion objective and ×15 ocular magnification, resulting in a total magnification of ×945. The Chroma 62002v2 filter set (Rockingham, VT) was employed for fluorescence excitation and emission. Images were acquired with a QImaging Retiga EX1 charge-coupled-device camera controlled by Openlab software (Improvision, Waltham, MA). Images were analyzed using ImageJ, version 1.37.

Transmission electron microscopy (TEM). Samples were fixed, prepared, and imaged as previously described (19).

Metabolic flux analysis. Metabolic flux calculations were performed using a previously developed model of *C. acetobutylicum* primary metabolism (10). Recent developments using a genetic algorithm improved model convergence in the presence of the nonlinearity (R. S. Senger and E. T. Papoutsakis, unpublished data).

RESULTS

LS FC analysis of sporulating cells [824(pSOS95del) and WT strains] identifies reproducible temporal patterns distinct from those of the asporogenous strain M5. (i) Analysis of sporulating strain 824(pSOS95del). We focused our initial investigations on cultures of 824(pSOS95del), which is an expression plasmid control strain and has been shown to sporulate in a large proportion of the culture compared to what is seen for the WT ATCC 824 strain (15). This phenomenon is shown to occur for all tested plasmid control strains due to host-plasmid interactions (38, 41). We examined the LS characteristics of three 824(pSOS95del) batch cultures (Fig. 1A and B), capturing the full sporulation program and metabolism

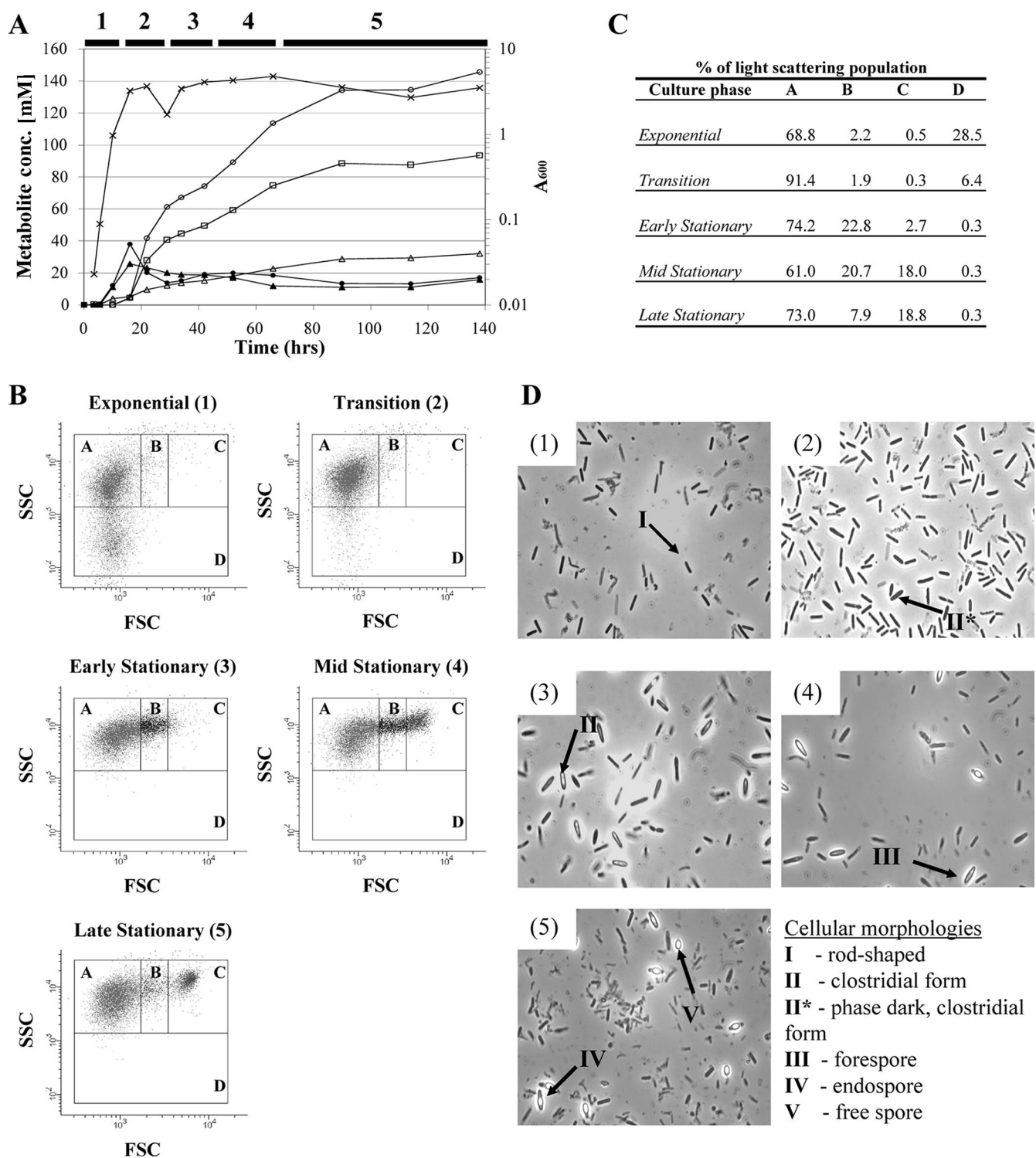


FIG. 1. LS investigation and metabolite analysis of a typical sporulating 824(pSOS95del) static flask culture. (A) Metabolite profiles, growth curves, and identification of batch culture stages. Symbols: \times , A_{600} ; \blacktriangle , acetate; \bullet , butyrate; \square , acetone; \triangle , ethanol; and \circ , butanol. Batch culture stages are identified by black bars as follows: 1, exponential; 2, transition; 3, early stationary; 4, mid-stationary; and 5, late stationary. (B) Dot plots from the LS (FSC/SSC) analysis. Dot plots were gated into four regions as follows: A, low FSC/high SSC; B, mid-FSC/high SSC; C, high FSC/high SSC; and D, all FSC/low SSC. (C) Composition of cell population for each LS region in the panel B dot plots shown as the percentage of total population. (D) Phase-contrast microscopy of the same sample analyzed by FC. Numbers on microscopy images correspond to the numbers on dot plots. Arrows point to the morphologies we are most interested in identifying and quantifying by FC. conc., concentration.

of *C. acetobutylicum* ATCC 824. LS samples were taken every 2 h during the exponential and transition phases, every 4 h during early stationary phase, every 6 to 12 h during mid-stationary phase, and every 12 to 24 h during the late stationary phase (Fig. 1A). FC analyses of three biological 824(pSOS95del) replicates revealed four unique cell populations, which are gated as follows: A, low-intensity FSC (low FSC)/high-intensity SSC (high SSC); B, middle-intensity FSC (mid-FSC)/high SSC; C, high FSC/high SSC; and D, all FSC/low SSC. FSC/SSC dot plots and corresponding phase-contrast microscopy from one representative 824(pSOS95del) culture are shown in Fig. 1B and D. Populations A and D were the two major populations during exponential growth, comprising 69% and 29% of the total population, respectively. Phase-contrast microscopy demonstrated that all cells were rod shaped and presumably vegetative. During the transition phase, the majority of cells (>91% of the total population) exhibited greater SSC intensity, condensing into population A. The majority of cells still appeared rod shaped and vegetative, but there was a very small emerging population of swollen, dark-phase cells, characteristic of the cigar-shaped, dark-phase clostridial-form cells (18, 22). As the culture progressed into early stationary phase, 23% of the population exhibited higher FSC intensity, as illustrated by the evolving population in gate B. Phase-contrast microscopy revealed the presence of clostridial-form cells (swollen, typically bright-phase morphologies) and forespore-containing cells (swollen morphologies, exhibiting a single, bright-phase end) in approximately one-fourth of the population. During mid-stationary phase, a population with FSC of even greater average intensity emerged, illustrated by the cells accumulating in gate C. The total cell population was distributed among gates A, B, and C as 61%, 21%, and 18% at this culture phase, respectively. Phase-contrast microscopy revealed the presence of rod-shaped cells, clostridial-form cells, forespore-containing cells, endospore-containing cells (bright-phase spores still surrounded by the mother cell), and free spores (very-bright-phase spheres). During late stationary phase, the majority of the population resolved in gates A and C, comprising 73% and 19% of the total population, respectively. A small percentage of cells exhibited gate B LS characteristics during late stationary phase (7.9%) compared to those exhibiting them during mid-stationary phase (20.7%). Phase-contrast microscopy revealed free spores, endospore-containing cells, and rod-shaped cells but few clostridial-form cells and forespore-containing cells compared to what was seen for early- and mid-stationary-phase samples. LS population percentages for each phase of growth are summarized in Fig. 1C.

This and biological replicate analyses suggest that the increasing mean FSC populations in gates B and C are representative of sporulating cells, more specifically, clostridial-form cells and forespore-containing cells in gate B and endospore-containing cells and free spores in gate C. To further substantiate our claim, we applied the same analysis to WT and M5 batch cultures.

(ii) Analysis of the sporulating WT and asporogenous M5 strains. For WT cultures, we expected the same LS characteristics as for of 824(pSOS95del) but as a smaller proportion of the total cell population (15). M5 does not sporulate and does not produce clostridial-form cells, and thus we do not expect to observe well-defined populations in gates B and C. Three bi-

ological replicates of WT and M5 strains were analyzed for LS characteristics as for the 824(pSOS95del) cultures. Dot plot samples are shown in Fig. S1A and B in the supplemental material. The same LS characteristics and temporal phenomena observed for 824(pSOS95del) cultures were apparent for WT cultures. Again, there was the condensation of cells into gate A, followed by the evolution of populations in gate B and then gate C, and finally the resolution of distinct populations in gates A and C that were not connected by a significant gate B population (Fig. 1B, "Late Stationary" panel). However, as expected (15), a smaller percentage of the total population was involved. For any WT sample, there were at most 14.7% and 8.8% of the total population measured in gates B and C, respectively, compared to 22.8% and 18.8% in gates B and C for a typical 824(pSOS95del) culture.

M5 cultures never displayed distinct populations in gates B and C at any time. They displayed an increase mean SSC intensity during the switch from exponential to transition phases, but beyond the transition phase, the cells either retained gate A LS characteristics or exhibited disperse and increased FSC-SSC intensities (Fig. 2). Interestingly, the observation of disperse, increased FSC-SSC intensity coincided with the end of metabolism, marked by the cessation in glucose consumption and metabolite production (Fig. 2). This was exhibited by all M5 cultures and other mutant strain cultures that prematurely ceased metabolism (data not shown).

NA (PI and Syto9) staining in combination with LS allows discrimination of all major sporulation-associated phenotypes, and FACS makes it possible to isolate highly enriched sporulation phenotypes. So far, our data have shown that LS alone is capable of distinguishing and quantifying sporulating from nonsporulating cells but that it does not clearly discriminate between the clostridial-form cells and forespore-containing cells (presumably gate B) or between endospore-containing cells and free spores (gate C). To solve this problem, we combined the LS assay with the Live/Dead *BacLight* viability assay. Although the *BacLight* assay's intended application is to distinguish between live and dead bacteria, several investigators have described ambiguous results in using this assay as a viability test (3, 17, 29, 36). In the context of clostridia or other endospore formers, the Live/Dead *BacLight* assay was used for analyzing vegetative *C. acetobutylicum* cultures via fluorescence microscopy, but results for sporulating phenotypes were not reported (16). We recently argued (19) that this assay cannot be used as a viability assay in this organism, but it can likely distinguish sporulation phenotypes.

We analyzed the same cell samples from the previously described 824(pSOS95del), WT, and M5 cultures. There were no obvious correlations between PI and Syto9 NA staining alone and sporulation phenotypes, but when gated upon the LS gates, we noticed distinct subpopulations in LS gates A, B, and C. As shown in Fig. 3A, two distinct NA staining populations resolved for the early-stationary-phase sample, which we gated as R1 (PI⁻/Syto9⁺) and R2 (PI⁺/Syto9^{dim}). For the total population, 34.3% and 43.8% of the cells were in gates R1 and R2, respectively. When gated upon LS region A, 27.4% and 48.3% of the cells were in gates R1 and R2, respectively. When gated upon LS region B, 50.1% and 33.5% of the cells were in gates R1 and R2, respectively. Thus, a noticeable enrichment for R1

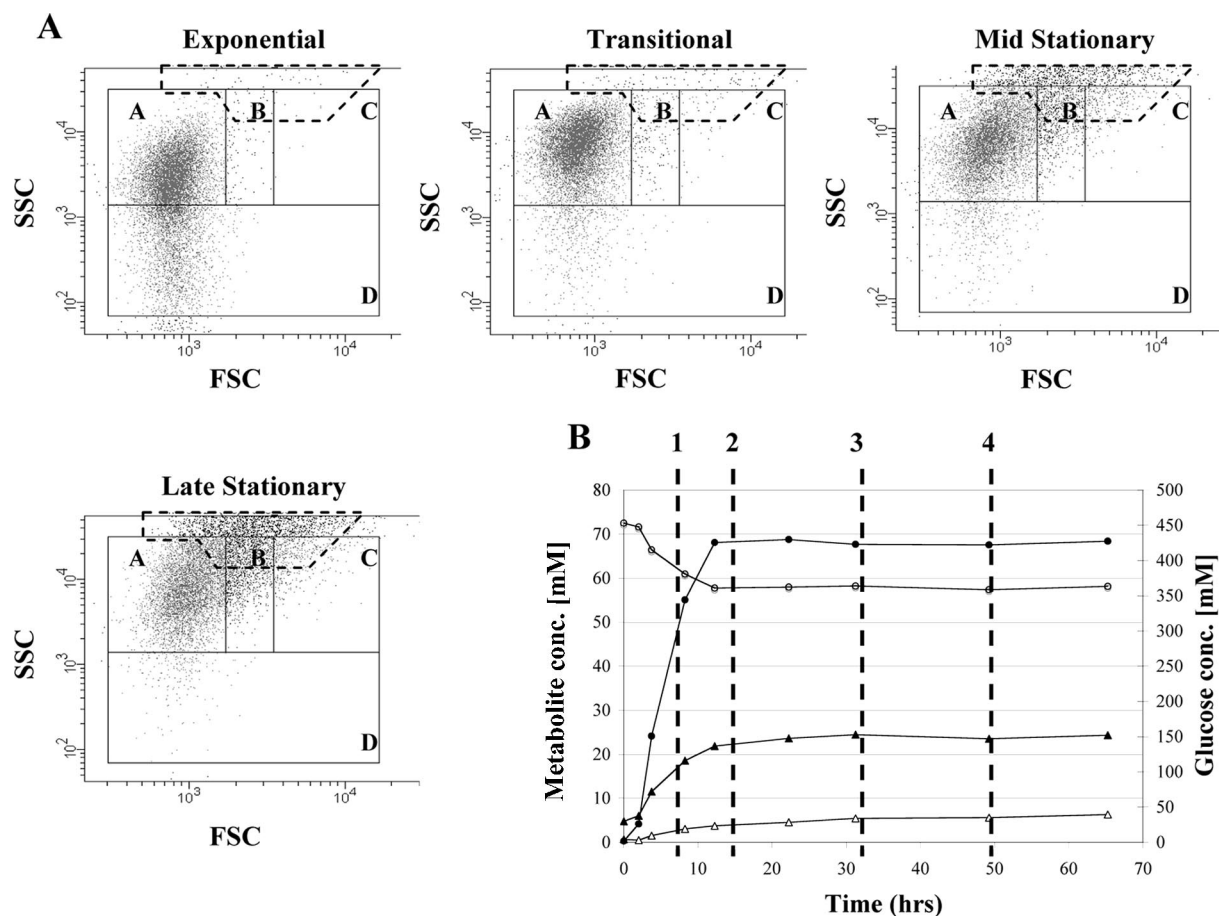


FIG. 2. LS characteristics of an asporogeneous M5 culture. (A) LS dot plots from various stages of the batch culture. The broken gate encompasses the disperse high-intensity FSC-SSC events, which are characteristic of a metabolically inactive culture and absent from an actively metabolizing culture. (B) Metabolite profiles and growth curve for a typical M5 batch culture. Symbols: \circ , glucose; \blacktriangle , acetate; \bullet , butyrate; and \triangle , ethanol. There was no measurable butanol or acetone. Samples corresponding to the dot plots in panel A are marked with numbers as follows: 1, exponential; 2, transition; 3, mid-stationary; and 4, late stationary. Notice that between hours 20 and 25, metabolite concentrations do not change appreciably, suggesting that the culture is no longer metabolically active. This corresponds to the time at which disperse high-intensity FSC-SSC events become more prevalent and the culture is unable to be serially cultured. conc., concentration.

(PI⁻/Syto9⁺) was witnessed in LS region B and likewise for R2 (PI⁻/Syto9^{dim}) in LS region A.

To more rigorously characterize these subpopulations, we employed FACS to sort and analyze cells via phase-contrast microscopy and TEM. We sorted at least 5 million cells from all four populations: R1, A; R2, A; R1, B; and R2, B. We found that 5 million events are necessary to obtain enough cells for efficient pelleting via high-speed centrifugation. As shown in Fig. 3B, there was enrichment for clostridial-form cells in R1, B; for forespore-containing cells in R1, A; and for rod-shaped cells in both R2, B and R2, A, presumably vegetative cells. The purity for each specific phenotype was never 100%, because sorting was performed at rates of $>80,000$ cells/s. Even at these rates, it still required ca. 5 h per sample to obtain 5 million cells for each population. Thus, for practical considerations, we sacrificed purity for large numbers of cells.

Enrichment for clostridial-form cells in LS gate B was expected, but enrichment for forespore-containing cells in LS gate A was not. Postsorting LS analysis of the enriched populations revealed the following mean FSC intensities: 2,028 for

R1, B (clostridial-form cells); 1,735 for R2, B (rod-shaped cells); 1,250 for R1, A (forespore-containing cells); and 1,037 for R2, A (rod-shaped cells). Gate B FSC bounds are 1,450 to 3,500, suggesting that clostridial-form cells and a small population of rod-shaped cells are captured in gate B. The forespore-containing cell population exists at the boundary between gates A and B, which we effectively distinguish from the bulk of rod-shaped, lower-FSC-intensity gate A cells via NA discrimination. However, to definitively capture forespore-containing cells and clostridial-form cells from the bulk of rod-shaped cells via LS discrimination alone, we extended the FSC lower bound of gate B to 1,200, sorted from the rest of the population, and imaged via TEM. Sorting for TEM analysis was performed at $<15,000$ cells/s to increase sample purity. Postsorting LS analysis revealed that the LS gate B population was enriched to 64% of the total population from 27% in the presorted population, and TEM imaging revealed that both clostridial-form cells (Fig. 4A) and forespore-containing cells (Fig. 4B) were the predominant morphologies.

In order to discriminate between endospore-containing cells

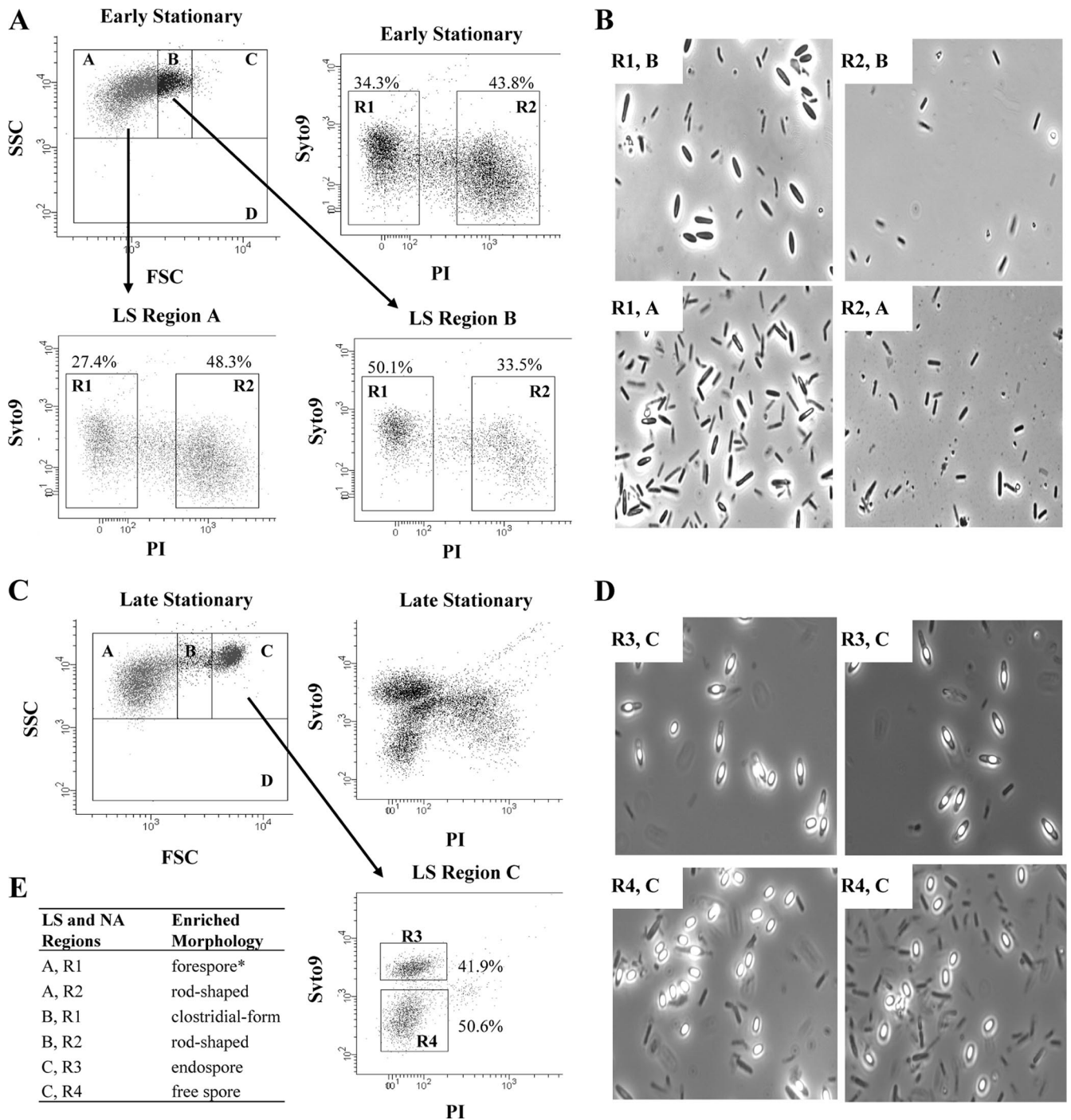


FIG. 3. Refinement of LS investigation with NA staining for both early- and late-stationary-phase samples of an 824(pSOS95del) batch culture. Populations were sorted based upon the combination of LS and NA staining characteristics. (A) LS and NA staining dot plots for an early-stationary-phase sample. We sorted the following four populations by FACS: R1, B ($PI^-/Syto^+$ and mid-FSC/high SSC); R2, B ($PI^+/Syto^{dim}$ and mid-FSC/high SSC); R1, A ($PI^-/Syto^+$ and low FSC/high SSC); and R2, A ($PI^+/Syto^{dim}$ and low FSC/high SSC). Percentages within each NA gate for the respective LS gate are indicated. (B) Microscopy of sorted populations from the early-stationary-phase sample. (C) LS and NA staining dot plots for the late-stationary-phase sample. The following two populations were sorted by FACS: R3, C ($Syto^+/PI^{dim}$ and high FSC/high SSC); and R4, C ($Syto^{dim}/PI^{dim}$ and high FSC/high SSC). The percentage within each NA gate for the respective LS gate C is indicated. (D) Microscopy of sorted populations from the late-stationary-phase sample. (E) Summary of the predominant morphologies for each sorted population. *, postsorting analysis revealed that forespore-containing cells exhibited LS characteristics very near the border of gates A and B. We expanded gate B and sorted again to show that gate B captures predominately clostridial-form cells and forespores (Fig. 4).

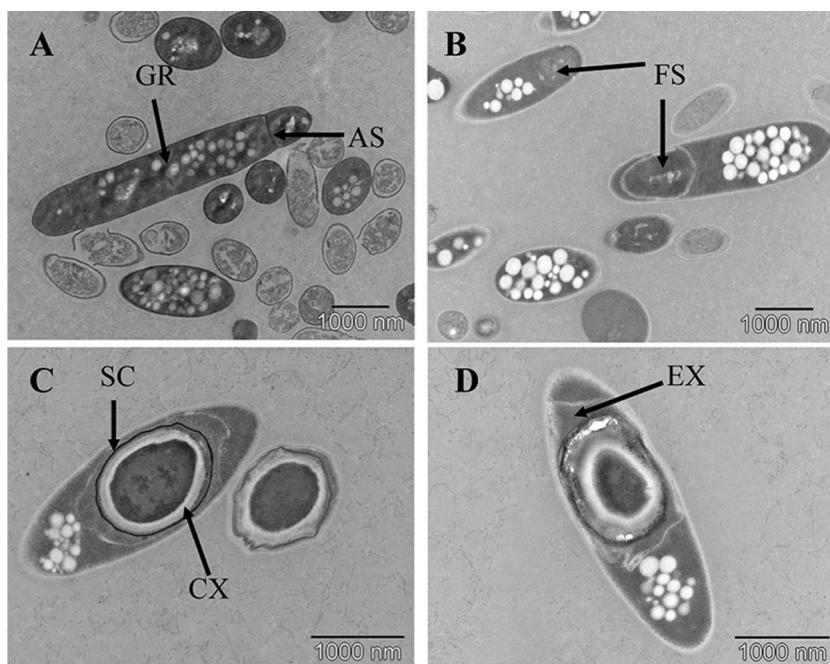


FIG. 4. TEM of sorted cells from LS gates B (panels A and B) and C (panels C and D) (refer to Fig. 3). Clostridial-form cells and forespore-containing cells were the predominant morphologies in all fields of view for LS gate B, and endospore-containing cells and free spores were predominant for LS gate C. (A) Clostridial-form cells with arrows pointing to granules (GR) and asymmetric septum formation (AS). (B) Forespore-containing cells, which all contained granules. Arrows are pointing to the developing forespore (FS). (C) Endospore-containing cells and free spores with arrows pointing to the spore coat (SC) and the spore cortex (CX). (D) Mature endospore-containing cell with what appears to be an exosporium (EX) surrounding the endospore.

and free spores, we performed NA staining on late-stationary-phase 824(pSOS95del) samples. Multiple NA staining populations resolved (Fig. 3C, top right), but upon gating upon LS region C, only two distinct populations remained (Fig. 3D, bottom right). We gated these as R3 ($PI^{dim}/Syto9^+$) and R4 ($PI^{dim}/Syto9^{dim}$), sorted, and imaged via phase-contrast microscopy. Phase-contrast microscopy revealed that $>75\%$ of R3, C-sorted cells were endospore-containing cells or free spores (top two images of Fig. 3D), and postsorting LS analysis revealed that 88% of sorted cells exhibited gate C LS characteristics. Significantly, microscopy analysis showed that $>90\%$ of the spore morphologies were endospore-containing cells.

Phase-contrast microscopy of R4, C-sorted cells suggested that $\sim 50\%$ of the cells display a spore morphology, of which $>95\%$ were free spores (bottom two images of Fig. 3D). FC postsorting analysis of R4, C cells revealed that 27% exhibited gate A, 5% gate B, and 68% gate C LS characteristics. The discrepancy between FC and microscopy postsorting analysis was likely due to poor microscope slide preparation, with many cells being out of the plane of focus. Thus, we sorted upon LS gate C characteristics only and analyzed by TEM to more rigorously characterize the sorted morphologies. Sorting was performed at $<15,000$ cells/s in order to increase sorted population purity. Postsorting analysis revealed that 91% of the cells exhibited LS gate C characteristics. Inspection of TEM images from LS gate C-sorted cells revealed that $>90\%$ of the morphologies were of either endospore-containing cells or free spores (Fig. 4C and D).

FC analysis provides precise temporal insight into sporulation and identifies multiple rounds of sporulation and spore germination in a single batch culture. We applied LS analysis to quantitatively assess sporulation kinetics. We first analyzed and compared batch cultures of 824(pMSPO0A), which is a Spo0A overexpression strain under its natural promoter (copy number, ca. 7), against those of the WT and 824(pSOS95del) strains. Spo0A is the master transcription regulator of both sporulation and solvent formation in clostridia, and upon overexpression during vegetative growth it is suggested to induce sporulation earlier than what is seen for both WT and 824(pSOS95del) cultures (15). In order to determine and accurately compare when sporulation begins, we accounted for differences in inocula and the lengths of lag phase by setting time zero ($t = 0$) as the time at which the batch culture reached an A_{600} value of 1.0. Distinct and defined populations in gates B and C appeared 9 hours and 15 hours early in the 824(pMSPO0A) culture compared to the average of three biological replicate 824(pSOS95del) and WT cultures, respectively (see Fig. S2 in the supplemental material). Our data also show that the 824(pSOS95del) initiates sporulation 6 hours earlier than WT and that for all cultures it takes approximately 10 to 14 h for clostridial-form cells to differentiate into endospore-containing cells.

LS analysis of these cultures also showed that batch *C. acetobutylicum* cultures can and often do carry out multiple rounds of sporulation. As shown in Fig. 5, top three graphs, the distinct gate C population (endospore-containing cells and free

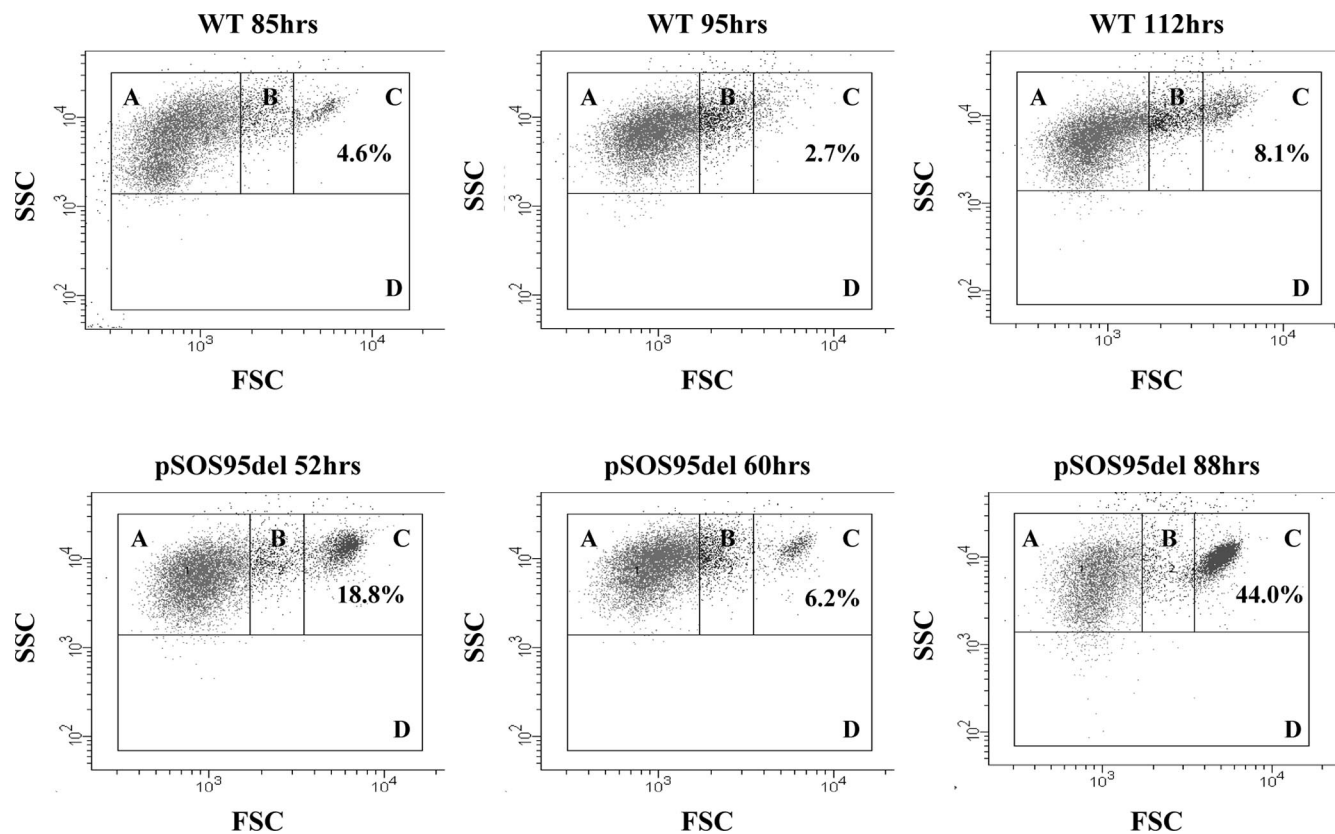


FIG. 5. Temporal analysis of batch culture sporulation for multiple strains of *C. acetobutylicum*, which proved multiple rounds of sporulation. Dot plots for typical WT (top row) and 824(pSOS95del) (bottom row) cultures showed that the endospore-containing cell/free spore population (gate C) develops, disappears, and then develops again as the culture ages. The percentage of cells within the entire population that exhibited gate C characteristics is provided on each dot plot. Our data demonstrated germination of spores, multiple rounds of sporulation, and synchrony for the first round of germination. Results were similar for all differentiating cultures analyzed (seven for this study).

spores) essentially disappeared from the WT culture between hours 85 and 95 and then reappeared 15 to 25 h later as a greater percentage of the total population. The same phenomena occurred for 824(pSOS95del) cultures. As shown in Fig. 5,

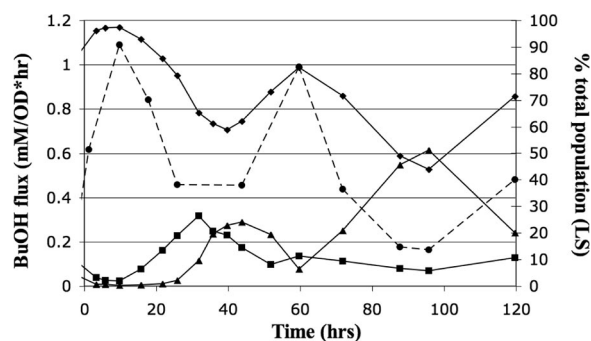


FIG. 6. Correlation between LS characteristics and butanol flux for 824(pSOS95del). Graphs are labeled with the following symbols: \blacklozenge plus a solid line, rod-shaped, vegetative population; \blacksquare plus a solid line, clostridial-form cell population; \blacktriangle plus a solid line, endospore-containing cell/free spore population; and \bullet plus a broken line, butanol flux. Notice that changes in butanol flux correlated directly with the changes in the percentage of vegetative cells and inversely with the percentage of clostridial-form cells. Decreases in endospore-containing cell/free spore population were indicative of germination, which correlated with increases in vegetative population and butanol flux. OD, optical density.

bottom three graphs, the percentage of cells exhibiting gate C characteristics was reduced from 18% to 6% of the total population between hours 52 and 60 and then reappeared as almost 50% of the total population 20 to 30 h later. These results suggest spore germination and multiple rounds of sporulation, which was previously suggested but not proven (38), and is in accordance with previous DNA microarray analyses (19). Additionally, the abrupt drop in spore population suggests synchronized germination. Multiple rounds of sporulation occurred in all but one of the sporulating batch cultures that we analyzed during this study (seven of eight total), and the phenotypes seen exhibited interesting correlations to culture metabolism, which we discuss next.

Correlation of LS-discriminated phenotypes to cellular metabolism: is the clostridial cell form responsible for solvent formation? Using *C. saccharobutylicum*, previously classified as *C. acetobutylicum* P262 (21), Jones et al. suggested from microscopic evidence that a correlation exists between the number of swollen, cigar-shaped clostridial-form cells and solvent production (18). Using chemical mutagenesis, they derived mutants unable to form clostridial-form cells, which did not produce solvents. Other mutants that displayed reduced granule accumulation produced intermediate levels of solvents, and mutants blocked at the clostridial-form cell phenotype produced WT levels of solvents. They concluded that clostridial-form cells were responsible for the conversion of acids to

solvents, which is now widely accepted for all solventogenic clostridia. Our data challenge this view for *C. acetobutylicum* ATCC 824.

By comparing butanol fluxes to LS populations, our data showed that the fraction of the vegetative, rod-shaped population is directly correlated to butanol flux; in contrast, the frequency of clostridial-form cells and of endospore-containing cells plus free spores is inversely correlated to butanol flux (Fig. 6). We determined butanol flux as the change in butanol concentration over time per unit biomass (in A_{600} units, as determined by optical density) (10). The fraction of vegetative cells and the butanol flux increased and decreased largely in synchrony. In contrast, the fraction of clostridial-form cells followed a largely opposite pattern in terms of butanol flux correlation through hour 50. The population of clostridial-form cells remained relatively constant from hour 50 on, while the fraction of the endospore-containing cell/free spore population continuously increased from hour 60 on. At hour 24, the endospore-containing cell/free spore population began to increase with an approximately 10- to 14-h lag behind the clostridial-form cell population and at the expense of clostridial-form cell population. The endospore-containing cell/free spore population reached a maximum for the first round of sporulation around hour 45 to hour 50 and then decreased, presumably due to germination. The germination process persisted for 10 to 15 h and was accompanied by increases in the percentage of vegetative cells and in butanol flux. A biological replicate 824(pSOS95del) batch culture exhibited the same phenomena, but with a less dramatic germination event and subsequently less of an impact on butanol flux (data not shown). Similar phenomena were observed for WT cultures (see Fig. S3 in the supplemental material) but were not as pronounced, since a smaller percentage of the culture sporulates. These data suggest that a vegetative cell phenotype is predominately responsible for butanol production, and such a vegetative cell phenotype is likely a precursor to clostridial-form cells.

DISCUSSION

We developed FC methods and demonstrated the ability to analyze *C. acetobutylicum* cultures faster, more precisely, and more quantitatively than ever before. By LS discrimination alone, we were able to detect the temporal aspects of sporulation, accurately quantify the proportion of the population participating in sporulation, and sort cultures into enriched populations for subsequent analysis. By coupling with NA staining, we effectively discriminated between all four major sporulation-associated phenotypes, and by using FACS, we were able to enrich for the various sporulation phenotypes. Finally, we demonstrated that previously supposed phenomena and new hypotheses could be more critically examined using FC. For example, using the FC LS assay, we detected and characterized multiple rounds of sporulation along with germination and early sporulation due to the overexpression of the Spo0A. Both phenomena were previously proposed (15, 38) but never proven or measured with such precision. We also determined that disperse high-intensity FSC-SSC events are characteristic of metabolically inactive cultures. We suggest that these events are due to doublets and triplets of lysed cells,

which could exhibit a stronger propensity to aggregate than nonlysed cells.

In addition to refining the LS assay, NA staining combined with LS revealed important physical and biochemical information about sporulation phenotypes and will make possible more-critical analysis of such phenotypes via FACS enrichment in the future. For example, the exclusion of all NA stains from the free spore but not the endospore in endospore-containing cells suggests an addition to the developing spore, likely the spore coat, which is responsible for Syto9 exclusion. Interestingly, our observation of Syto9 and PI exclusion by free spores and partial exclusion by endospores is similar to that reported for the analysis of *Bacillus cereus* endospore germination via Syto9 staining (9) and identical to results for Syto13 and PI staining of *Paenibacillus polymyxa* (7). Also, the exclusion of PI from clostridial-form cells and forespore-containing cells but not from the majority of rod-shaped cells and the mother cell compartments of the endospore-containing cells suggests a physical difference in the cell membranes of these phenotypes. Cell membrane composition changes are a well-known fact in *C. acetobutylicum* and other solventogenic clostridia. Particularly during the metabolic shift from acidogenesis to solventogenesis, cells compensate for the increase of membrane fluidity associated with increased butanol concentration by increasing the proportion of saturated fatty acids and the mean acyl chain length in the cell membrane (37, 44). However, this knowledge comes from heterogeneous cultures, and little is known about specific phenotypes. We demonstrated that FACS can be employed to rapidly purify and quantify all sporulation populations for subsequent detailed TEM analysis and should be able to complement other single-cell analyses, such as Raman and Fourier transform infrared spectroscopy (31–33), which precisely measure membrane composition, DNA content, and RNA content, etc.

To conclude our discussion of method development, we applied these techniques to investigate the relationship between morphology and solvent production. We showed that correlations between LS analyses and metabolite production for both WT and 824(pSOS95del) batch cultures strongly suggest that the clostridial-form cells do not produce solvent and actually detract from solvent production. Subsequently, we proposed that a clostridial-form cell precursor is actually the major solvent producer, which challenges a long-accepted belief that clostridial-form cells are the major solvent producer in all solventogenic clostridial cultures.

Although we report only on the analysis of four *C. acetobutylicum* strains, we applied our methods to several other recombinant strains and do not foresee why such methods cannot be immediately applied to all clostridial species. However, extra care should be taken in the analysis of pathogenic species such as *C. botulinum*, so that no aerosolized toxin is generated during FC analysis. Given the tremendous interest in clostridial cell culture, we look forward to the application of FC techniques for accelerating research on various industrially significant clostridial species (*C. acetobutylicum*, *C. thermocellum*, *C. cellulolyticum*, *C. phytofermentans*, and *C. beijerinckii*, etc.) and for advancing the study of pathogenic species (*C. botulinum*, *C. difficile*, *C. perfringens*, and *C. tetani*, etc.).

ACKNOWLEDGMENTS

We acknowledge the use of the Northwestern University Biological Imaging Facility for the light microscopy and Shannon Modla at the Delaware Biotechnology Institute Bio-Imaging Facility for the electron microscopy. We also acknowledge James Marvin from the Robert H. Lurie Comprehensive Cancer Center FC Core Facility at Northwestern University for initial cell sorting experiments.

Work was supported by an NSF grant (BES-0418157/CBET-0824629) and an NIH/NIGMS biotechnology training grant (T32-GM08449) fellowship for Bryan P. Tracy.

REFERENCES

- Avery, S. V. 2006. Microbial cell individuality and the underlying sources of heterogeneity. *Nat. Rev. Microbiol.* **4**:577–587.
- Balaban, N. Q., J. Merrin, R. Chait, L. Kowalik, and S. Leibler. 2004. Bacterial persistence as a phenotypic switch. *Science* **305**:1622–1625.
- Berney, M., F. Hammes, F. Bosshard, H. U. Weilenmann, and T. Egli. 2007. Assessment and interpretation of bacterial viability by using the LIVE/DEAD BacLight kit in combination with flow cytometry. *Appl. Environ. Microbiol.* **73**:3283–3290.
- Brehm-Stecher, B. F., and E. A. Johnson. 2004. Single-cell microbiology: tools, technologies, and applications. *Microbiol. Mol. Biol. Rev.* **68**:538.
- Clark, S. W., G. N. Bennett, and F. B. Rudolph. 1989. Isolation and characterization of mutants of *Clostridium acetobutylicum* ATCC 824 deficient in acetoacetyl-coenzyme A:acetate/butyrate:coenzyme A-transferase (EC 2.8.3.9) and in other solvent pathway enzymes. *Appl. Environ. Microbiol.* **55**:970–976.
- Claverys, J. P., and L. S. Havarstein. 2007. Cannibalism and fratricide: mechanisms and raisons d'être. *Nat. Rev. Microbiol.* **5**:219–229.
- Comas-Riu, J., and J. Vives-Rego. 2002. Cytometric monitoring of growth, sporogenesis and spore cell sorting in *Paenibacillus polymyxa* (formerly *Bacillus polymyxa*). *J. Appl. Microbiol.* **92**:475–481.
- Cornillot, E., R. V. Nair, E. T. Papoutsakis, and P. Soucaille. 1997. The genes for butanol and acetone formation in *Clostridium acetobutylicum* ATCC 824 reside on a large plasmid whose loss leads to degeneration of the strain. *J. Bacteriol.* **179**:5442–5447.
- Cronin, U. P., and M. G. Wilkinson. 2007. The use of flow cytometry to study the germination of *Bacillus cereus* endospores. *Cytometry A* **71A**:143–153.
- Desai, R. P., L. K. Nielsen, and E. T. Papoutsakis. 1999. Stoichiometric modeling of *Clostridium acetobutylicum* fermentations with non-linear constraints. *J. Biotechnol.* **71**:191–205.
- Dürre, P. 2005. Clostridial enterotoxins (genetics), p. 659–669. *In* P. Dürre (ed.), *Handbook on clostridia*, vol. 1. Taylor & Francis Group, LLC, Boca Raton, FL.
- Gilmore, M. S., and W. Haas. 2005. The selective advantage of microbial fratricide. *Proc. Natl. Acad. Sci. USA* **102**:8401–8402.
- Gonzalez-Pastor, J. E., E. C. Hobbs, and R. Losick. 2003. Cannibalism by sporulating bacteria. *Science* **301**:510–513.
- Haraldsen, J. D., and A. L. Sonenshein. 2003. Efficient sporulation in *Clostridium difficile* requires disruption of the σ^K gene. *Mol. Microbiol.* **48**:811–821.
- Harris, L. M., N. E. Welker, and E. T. Papoutsakis. 2002. Northern, morphological, and fermentation analysis of *spo0A* inactivation and overexpression in *Clostridium acetobutylicum* ATCC 824. *J. Bacteriol.* **184**:3586–3597.
- Hillmann, F., R. J. Fischer, and H. Bahl. 2006. The rubrerythrin-like protein Hsp21 of *Clostridium acetobutylicum* is a general stress protein. *Arch. Microbiol.* **185**:270–276.
- Hoefel, D., W. L. Grooby, P. T. Monis, S. Andrews, and C. P. Saint. 2003. Enumeration of water-borne bacteria using viability assays and flow cytometry: a comparison to culture-based techniques. *J. Microbiol. Methods* **55**:585–597.
- Jones, D. T., A. van der Westhuizen, S. Long, E. R. Allcock, S. J. Reid, and D. R. Woods. 1982. Solvent production and morphological changes in *Clostridium acetobutylicum*. *Appl. Environ. Microbiol.* **43**:1434–1439.
- Jones, S. W., C. J. Paredes, B. P. Tracy, N. Cheng, R. Sillers, R. S. Senger, and E. T. Papoutsakis. 2008. The transcriptional program underlying the physiology of clostridial sporulation. *Genome Biol.* **9**:R114.
- Junne, S., E. Klein, A. Angersbach, and P. Goetz. 2008. Electrooptical measurements for monitoring metabolite fluxes in acetone-butanol-ethanol fermentations. *Biotechnol. Bioeng.* **99**:862–869.
- Keis, S., R. Shaheen, and D. T. Jones. 2001. Emended descriptions of *Clostridium acetobutylicum* and *Clostridium beijerinckii*, and descriptions of *Clostridium saccharoperbutylacetonicum* sp. nov. and *Clostridium saccharobutylicum* sp. nov. *Int. J. Syst. Evol. Microbiol.* **51**:2095–2103.
- Long, S., D. T. Jones, and D. R. Woods. 1983. Sporulation of *Clostridium acetobutylicum* P262 in a defined medium. *Appl. Environ. Microbiol.* **45**:1389–1393.
- Lynd, L. R., W. H. van Zyl, J. E. McBride, and M. Laser. 2005. Consolidated bioprocessing of cellulosic biomass: an update. *Curr. Opin. Biotechnol.* **16**:577–583.
- Lynd, L. R., P. J. Weimer, W. H. van Zyl, and I. S. Pretorius. 2002. Microbial cellulose utilization: fundamentals and biotechnology. *Microbiol. Mol. Biol. Rev.* **66**:506.
- Minton, N. P. 2003. Clostridia in cancer therapy. *Nat. Rev. Microbiol.* **1**:237–242.
- Paredes, C. J., K. V. Alsaker, and E. T. Papoutsakis. 2005. A comparative genomic view of clostridial sporulation and physiology. *Nat. Rev. Microbiol.* **3**:969–978.
- Philippe, V. A., M. B. Mendez, I. H. Huang, L. M. Orsaria, M. R. Sarker, and R. R. Grau. 2006. Inorganic phosphate induces spore morphogenesis and enterotoxin production in the intestinal pathogen *Clostridium perfringens*. *Infect. Immun.* **74**:3651–3656.
- Popoff, M. R., and B. R. Stiles. 2005. Clostridial toxins vs. other bacterial toxins, p. 323–383. *In* P. Dürre (ed.), *Handbook on clostridia*, vol. 1. Taylor & Francis Group, LLC, Boca Raton, FL.
- Sachidanandham, R., K. Y. Gin, and C. L. Poh. 2005. Monitoring of active but non-culturable bacterial cells by flow cytometry. *Biotechnol. Bioeng.* **89**:24–31.
- Schuster, K. C., R. Goodacre, J. R. Gapes, and M. Young. 2001. Degeneration of solventogenic *Clostridium* strains monitored by Fourier transform infrared spectroscopy of bacterial cells. *J. Ind. Microbiol. Biotechnol.* **27**:314–321.
- Schuster, K. C., F. Mertens, and J. R. Gapes. 1999. FTIR spectroscopy applied to bacterial cells as a novel method for monitoring complex biotechnological processes. *Vib. Spectrosc.* **19**:467–477.
- Schuster, K. C., I. Reese, E. Urlaub, J. R. Gapes, and B. Lendl. 2000. Multidimensional information on the chemical composition of single bacterial cells by confocal Raman microspectroscopy. *Anal. Chem.* **72**:5529–5534.
- Schuster, K. C., E. Urlaub, and J. R. Gapes. 2000. Single-cell analysis of bacteria by Raman microscopy: spectral information on the chemical composition of cells and on the heterogeneity in a culture. *J. Microbiol. Methods* **42**:29–38.
- Shapiro, H. M. 2003. *Practical flow cytometry*, 4th ed., p. 514–516. John Wiley & Sons, Inc., Hoboken, NJ.
- Shapiro, H. M. 2000. Microbial analysis at the single-cell level: tasks and techniques. *J. Microbiol. Methods* **42**:3–16.
- Stocks, S. M. 2004. Mechanism and use of the commercially available viability stain, BacLight. *Cytometry A* **61**:189–195.
- Tomas, C. A., J. Beamish, and E. T. Papoutsakis. 2004. Transcriptional analysis of butanol stress and tolerance in *Clostridium acetobutylicum*. *J. Bacteriol.* **186**:2006–2018.
- Tomas, C. A., N. E. Welker, and E. T. Papoutsakis. 2003. Overexpression of *groESL* in *Clostridium acetobutylicum* results in increased solvent production and tolerance, prolonged metabolism, and changes in the cell's transcriptional program. *Appl. Environ. Microbiol.* **69**:4951–4965.
- Tsien, R. Y. 1998. The green fluorescent protein. *Annu. Rev. Biochem.* **67**:509–544.
- Tummala, S. B., N. E. Welker, and E. T. Papoutsakis. 2003. Design of antisense RNA constructs for downregulation of the acetone formation pathway of *Clostridium acetobutylicum*. *J. Bacteriol.* **185**:1923–1934.
- Walter, K. A., L. D. Mermelstein, and E. T. Papoutsakis. 1994. Studies of recombinant *Clostridium acetobutylicum* with increased dosages of butyrate formation genes. *Ann. N. Y. Acad. Sci.* **721**:69–72.
- Wiesenborn, D. P., F. B. Rudolph, and E. T. Papoutsakis. 1988. Thiolase from *Clostridium acetobutylicum* ATCC 824 and its role in the synthesis of acids and solvents. *Appl. Environ. Microbiol.* **54**:2717–2722.
- Worner, K., H. Szurmant, C. Chiang, and J. A. Hoch. 2006. Phosphorylation and functional analysis of the sporulation initiation factor Spo0A from *Clostridium botulinum*. *Mol. Microbiol.* **59**:1000–1012.
- Zhao, Y. S., L. A. Hindorf, A. Chuang, M. Monroe-Augustus, M. Lyristis, M. L. Harrison, F. B. Rudolph, and G. N. Bennett. 2003. Expression of a cloned cyclopropane fatty acid synthase gene reduces solvent formation in *Clostridium acetobutylicum* ATCC 824. *Appl. Environ. Microbiol.* **69**:2831–2841.